An Enhanced Total-Field/Scattered-Field Scheme for the 3-D Nonstandard Finite-Difference Time-Domain Method

Tadao Ohtani[1], Yasushi Kanai[2], and Nikolaos V. Kantartzis[3]

[1]1-17-134 Omachi, Asahikawa 070-0841, Japan, bytcg100@ybb.ne.jp
[2]Niigata Institute of Technology, Kashiwazaki 945-1195, Japan, kanai@iee.niit.ac.jp
[3]Aristotle University of Thessaloniki, GR-54124 Thessaloniki, Greece, kant@auth.gr

The nonstandard (NS)-FDTD method exhibits high accuracy at fixed frequencies and thus proven to be a powerful means for the radar cross section (RCS) analysis of scattering objects with complex shapes and materials. To this aim, significant enhancement can be pursued in the combination with the FDTD total-field/scattered-field (TF/SF) concept. However, the principal implementation characteristics of the latter in the NS-FDTD technique have not been yet elaborately studied, especially for electrically large domains or structures. Thus, in this paper, a new advanced TF/SF scheme for the 3-D NS-FDTD algorithm is developed and fully investigated. Numerical results reveal that the proposed method, considering the features of the NS-FDTD operators, is far more efficient and versatile than the original FDTD one.

***Index Terms*—Computational electromagnetics, electromagnetic propagation, finite difference methods, radar cross-sections.**

I. Introduction

The nonstandard finite-difference time-domain (NS-FDTD) technique is an advanced computational scheme with high isotropy and accuracy at specific frequencies [1]. Mainly, the method offers an intuitive numeration on Yee's cell according to the main FDTD concept. So, it can be deemed suitable for the scattering analysis of electrically large objects [2]-[6], like the radar cross section (RCS) of aircrafts with complex geometry and material configuration. In fact, this asset has been especially instructive for the design of modern devices. Essentially, to obtain RCS, it is necessary to extract the scattered from the total field in the FDTD domain. To this goal, the total-field/scattered-field (TF/SF) formulation has been widely used in conjunction with the FDTD framework [6]. However, the incorporation of the TF/SF features in the NS-FDTD method has not been sufficiently studied for prior problems. Based on these aspects, an enhanced TF/SF approach is introduced for the 3-D NS-FDTD algorithm in this paper. The novel formulation is found to outperform the usual FDTD counterpart, both in accuracy and efficiency, as validated by various demanding applications.

II. Development of The NS-FDTD TF/SF Technique

The NS-FDTD method uses two finite-difference (FD) operators with complementary error properties for *H*- and *E*-field calculations. Hence, we consider two different FD operators in the proposed TF/SF separation process, as well. In this context, the assumed-known incident fields at the TF/SF separation positions of our scheme are as follows: (a) update of $\mathbf{E}^n$,

$$(\mathbf{E},\mathbf{H})^n_{\text{analytical}} = (E_0, H_0)\, e^{j(\omega n\Delta t - \mathbf{k}_{\text{num}}\cdot\mathbf{r})}, \tag{1}$$

$$\mathbf{H}^{n+1/2}_{\text{subcal}} = \mathbf{H}^{n-1/2}_{\text{subcal}} - \nabla^{(0)} \times \mathbf{E}^{n}_{\text{analytical}}, \tag{2}$$

$$\mathbf{H}^{n+1/2}_{\text{assumed-known inc}} \Leftarrow \mathbf{H}^{n+1/2}_{\text{subcal}}, \tag{3}$$

and (b) update of $\mathbf{H}^{n-1/2}$

$$\mathbf{H}^{n-1/2}_{\text{subcal}} = \mathbf{H}^{n-3/2}_{\text{subcal}} - \nabla^{(0)} \times \mathbf{E}^{n-1}_{\text{analytical}}, \tag{4}$$

$$\mathbf{E}^{n}_{\text{subcal}} = \mathbf{E}^{n-1}_{\text{subcal}} + \nabla^{(1)} \times \mathbf{H}^{n-1/2}_{\text{subcal}}, \tag{5}$$

$$\mathbf{E}^{n}_{\text{assumed-known inc}} \Leftarrow \mathbf{E}^{n}_{\text{subcal}}. \tag{6}$$

In (1)-(6), n is the time step, $j^2 = -1$, ω the angular frequency, Δt the time increment, $\mathbf{k}_{\text{num}}$ the numerical wave-number in the NS-FDTD method [7], $\mathbf{r}$ the position vector, (E_0, H_0) are the amplitudes, and ($\mathbf{E}$, $\mathbf{H}$)$_{\text{subcal}}$ vectors calculated separately from NS-FDTD calculation itself. Moreover, $\nabla^{(0)}$ and $\nabla^{(1)}$ are the NS-FDTD operators, defined as

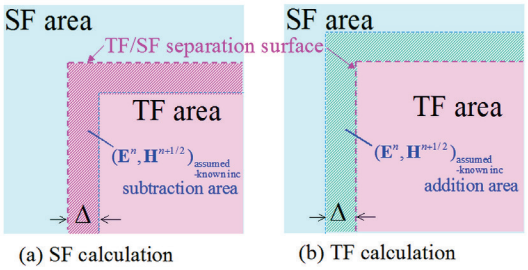

Fig. 1. Construction of the proposed NS-FDTD TF/SF scheme.

$$\nabla^{(*)} = \left[d_x^{(*)}/S_k(\Delta_x),\, d_y^{(*)}/S_k(\Delta_y),\, d_z^{(*)}/S_k(\Delta_z) \right], \tag{7}$$

$$d_\tau^{(0)} = \alpha_1 d_\tau^{(1)} + \alpha_2 d_\tau^{(2)} + \alpha_3 d_\tau^{(3)}, \tag{8}$$

where $\alpha_{1,2,3}$ are the isotropic wave propagation parameters for $\Sigma\alpha_i = 1$, $S_k(\Delta_\tau) = 2\sin(k\Delta_\tau/2)/k$ the spatial correction functions for Δ_τ and physical wave-number k used by the NS-FD method [1], and $d_x^{(*)}$ the FD operators along x-axis (similarly for $d_{y,z}^{(*)}$)

$$d_x^{(1)} f(x,y,z) = f(x+\tfrac{1}{2}\Delta_x, y, z) - f(x-\tfrac{1}{2}\Delta_x, y, z), \tag{9}$$

$$d_x^{(2)} f(x,y,z) = \sum_{\pm\text{sign}} \Big[f(x+\tfrac{1}{2}\Delta_x, y\pm\Delta_y, z\pm\Delta_z) - f(x-\tfrac{1}{2}\Delta_x, y\pm\Delta_y, z\pm\Delta_z) \Big] / 4, \tag{10}$$

$$d_x^{(3)} f(x,y,z) = \sum_{\pm\text{sign}} \Big[f(x+\tfrac{1}{2}\Delta_x, y\pm\Delta_y, z) - f(x-\tfrac{1}{2}\Delta_x, y\pm\Delta_y, z) + f(x+\tfrac{1}{2}\Delta_x, y, z\pm\Delta_z) - f(x-\tfrac{1}{2}\Delta_x, y, z\pm\Delta_z) \Big] / 4. \tag{11}$$

Note that if in (3) and (6) for the ($\mathbf{E}^n$, $\mathbf{H}^{n+1/2}$)$_{\text{assumed-known inc}}$ values we utilize ($\mathbf{E}^n$, $\mathbf{H}^{n+1/2}$)$_{\text{analytical}}$ instead of ($\mathbf{E}^n$, $\mathbf{H}^{n+1/2}$)$_{\text{subcal}}$, our generalized TF/SF model leads to the regular FDTD one. As depicted in Fig. 1, the scheme of (1)-(6) is applied only around the TF/SF separation surface. Thus, the computational burden of the new formulation is less than that required for the NS-FDTD calculation procedure itself in 3-D simulations.

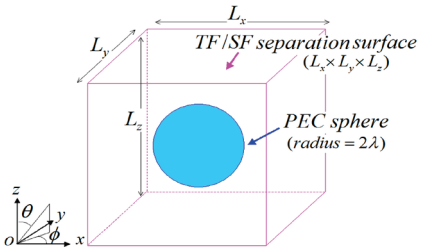

Fig. 2. Verification model of the proposed TF/SF scheme for $L_x = L_y = L_z = 6\lambda$. The PEC sphere is modeled via an aggregate of cubic cells with a width of Δ.

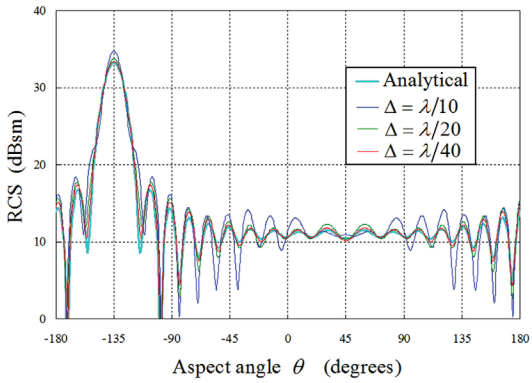

Fig. 3. Comparative bistatic RCS results for the PEC sphere of Fig. 2 with $\lambda = 1$ m. The direction of the incident plane wave is $\theta^{inc} = 45^o$, $\phi^{inc} = 0^o$, and $\phi^{Aspect} = 0^o$.

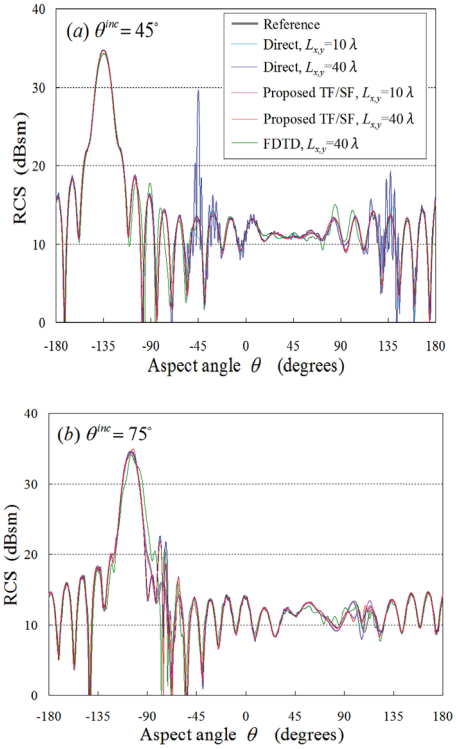

Fig. 4. Bistatic RCS for the PEC sphere of Fig. 2 with $\lambda = 1$ m in an electrically large area. The direction of the incident wave is $\phi^{inc} = 0^o$ and $\phi^{Aspect} = 0^o$.

III. Numerical Results – Discussion

Since the optimal accuracy of the NS-FDTD method is attained through cubic cells, we discretize the domain of Fig. 2 with such a grid and calculate the bistatic radar cross section (RCS), for an incident E_θ^{inc} generated by an airborne radar.

A. Verification of the enhanced TF/SF scheme

The target in Fig. 2 is a sphere of radius 2λ, comprising a perfect electric conductor (PEC) medium. After its 3-D NS-FDTD simulation combined with our TF/SF scheme, Fig. 3 gives the bistatic RCS results, where the analytical solution comes from a sphere with a smooth surface [8]. Note that the evaluated cell sizes vary as $\Delta = \lambda/10$ to $\lambda/40$. Evidently, the agreement with the analytical outcome increases as the lattice becomes finer, a fact which proves the validity of our TF/SF formulation. Also, considering the accuracy of the NS-FDTD method, it can be concluded that the computed results attain a sufficient staircase approximation of the sphere via the Δ cells.

B. TF/SF implementation in electrically large regions

Next, the novel TF/SF scheme is applied to the bistatic RCS analysis of the PEC sphere in an electrically large area with $\Delta = \lambda/10$, $L_x = L_y = 10\lambda$ and 40λ, and $L_z = 6\lambda$. For our validation, the result of Fig. 2 with $\Delta = \lambda/10$ is used as a reference. In this context, Fig. 4 presents the results, where "Direct" in the legend indicates that the outcomes were obtained by means of $(\mathbf{E}^n, \mathbf{H}^{n+1/2})_{\text{analytical}}$ instead of $(\mathbf{E}^n, \mathbf{H}^{n+1/2})_{\text{subcal}}$ in (3) and (6). As observed, both our TF/SF and "Direct" plots are in very good coincidence with the reference results for the $L_{x,y} = 10\lambda$ case. However, for $L_{x,y} = 40\lambda$, the "Direct" solution generates some undesired scattering waves at $\theta \approx -45^o$, 135^o, -75^o, and 105^o. Moreover, in the FDTD solution a noticeable pattern distortion arises. Overall, the featured algorithm outperforms the "Direct" and the FDTD scheme, yet it exhibits some slight discrepancies at $\theta \approx -75^o$ and 105^o, as shown in Fig. 4(b). Hence, particular attention is required for the choice of the reflection directions on the TF/SF separation surface. To eliminate these artifacts, the scattered field is calculated separately without the target and then subtracted from the result in the presence of the target. Although this process is steady, it needs twice the overhead of a typical simulation and hence it should be used only at particular observation angles. The prior analysis certifies the efficiency of the advanced 3-D NS-FDTD TF/SF technique and justifies its potential applicability in even more demanding configurations.

IV. References

[1] J. B. Cole, "High-accuracy Yee algorithm based on nonstandard finite differences: New developments and verifications," *IEEE Trans. Antennas Propag.*, vol. 50, no. 9, pp. 1185–1191, Sep. 2002.

[2] S. Koch, H. Schneider, and T. Weiland, "A low-frequency approximation to the Maxwell equations simultaneously considering inductive and capacitive phenomena," *IEEE Trans. Magn.*, vol. 48, no. 2, pp. 511–514, Feb. 2012.

[3] S. Ikuno, Y. Fujita, Y. Hirokawa, T. Itoh, S. Nakata, and A. Kamitani, "Large-scale simulation of electromagnetic wave propagation using meshless time domain method with parallel processing," *IEEE Trans. Magn.*, vol. 49, no. 5, pp. 1613–1616, May 2013.

[4] D. Schmidthausler, S. Schops, and M. Clemens, "Linear subspace reduction for quasistatic field simulations to accelerate repeated computations," *IEEE Trans. Magn.*, vol. 50, no. 2, art. no. 7010304, Feb. 2014.

[5] Y. El-Kurdi, W. Gross, and D. Giannacopoulos, "Parallel multigrid acceleration for the finite-element Gaussian belief propagation algorithm," *IEEE Trans. Magn.*, vol. 50, no. 2, art. no. 7014304, Feb. 2014.

[6] A. Taflove and S. Hagness, *Computational Electrodynamics: The Finite-Difference Time-Domain Method*. Norwood, MA: Artech House, 2005.

[7] T. Ohtani and Y. Kanai, "Optimal coefficients of the spatial finite difference operator for the complex nonstandard finite difference time domain method," *IEEE Trans. Magn.*, vol. 47, no. 5, pp. 1498–1501, May 2011.

[8] C. A. Balanis, *Advanced Engineering Electromagnetics,* New York, NY: Wiley, 2012.